Glycoconjugate Journal (1998) **15:** 183–186

EGC2

MMC and LD simulations of *α*-D-Man*p*-(1 → 2)-*β*-D-Glc*p*-OMe: comparison to long-range heteronuclear NMR coupling constants and to the crystal structure

Christer Höög and Göran Widmalm

Department of Organic Chemistry, Arrhenius Laboratory, Stockholm University, S-106 91 Stockholm, Sweden

The conformational flexibility and the dynamics of *α*-D-Man*p*-(1 → 2)-*β*-D-Glc*p*-OMe have been investigated by Metropolis Monte Carlo (MMC) and Langevin dynamics (LD) simulations. The two simulation techniques employ different force fields, namely the HSEA force field and a CHARMm-based force field. The former shows less conformational flexibility than the latter, in which a multiple energy minima conformational space is sampled. Long-range heteronuclear nuclear magnetic resonance (NMR) coupling constants have been measured by selective excitations of the carbons at the glycosidic linkage. Calculated $^3J_{C,H}$ values from MMC and LD simulations show excellent agreement to those from NMR experiments. The X-ray crystal structure has a conformation within a region of the conformational space populated in both force fields.

Keywords: **disaccharide, conformation, flexibility, HSEA, CHARMm**

Abbreviations: **CHARMm, Chemistry at HARvard Molecular Mechanics; FID, free induction decay; HSEA, hard sphere exo anomeric; LD, Langevin dynamics; MMC, Metropolis Monte Carlo; NMR, nuclear magnetic resonance**

Introduction

Carbohydrates are involved in biological processes such as cell–cell interactions, protein trafficking and regulation. They act as receptors on cell surfaces or as antigenic determinants on bacterial surfaces. These interactions are dependent on the specific three-dimensional structure of the carbohydrate. Variations of the chirality of a certain hydroxyl group, changes of the anomeric configuration or deoxygenation lead to different possibilities for interactions. The conformational flexibility and the dynamics are additional variables in the description of carbohydrate structures.

For investigation of their three-dimensional structure, nuclear magnetic resonance (NMR) spectroscopy, molecular modelling and, if possible, X-ray crystallography are techniques commonly used. We describe here the conformational flexibility of α-D-Man*p*-(1 → 2)-*β*-D-Glc*p*-OMe (Figure 1) investigated by Metropolis Monte Carlo (MMC) and Langevin dynamics (LD) simulations. Long-range heteronuclear NMR coupling constants have been measured across the glycosidic linkage and are compared to those calculated from simulations. The results from molecular modelling are also compared to the X-ray crystal structure of the compound.

Materials and Methods

Simulation

Simulations of α-D-Man*p*-(1 → 2)-*β*-D-Glc*p*-OMe [1] were performed on Silicon Graphics Inc. workstations. The torsional angles across the glycosidic linkage are defined as follows: ϕ: H1′-C1′-O2-C2 and ψ: C1′-O2-C2-H2, where the atoms of the mannosyl group are primed. Simulations were performed at 300 K. The GEGOP program, version 2.6, which uses the HSEA force field [2] was used for the Metropolis Monte Carlo (MMC) simulations [3] which employed 1 000 000 macro steps with a total acceptance ratio of 44%. The maximum step length for the glycosidic dihedral angles, ϕ and ψ, was set to 20°.

LD simulations were used to simulate the effects of solvent water [4] and performed using Quanta/CHARMm (Molecular Simulations Inc., San Diego, CA, USA) version 4.0 and PARM22. LD includes a collision frequency $\gamma = \zeta/m$, where ζ is the friction constant and m the atomic mass. A value of $\gamma = 50$ per ps was applied to carbons and oxygens. Two 5 ns runs with different seeds were performed using a time step of 1.0 fs and a constant dielectric of unity. Data were saved every 0.01 ps for analysis.

Low energy regions were identified from scatter plots of MMC and LD simulations. Energy minimization, using the

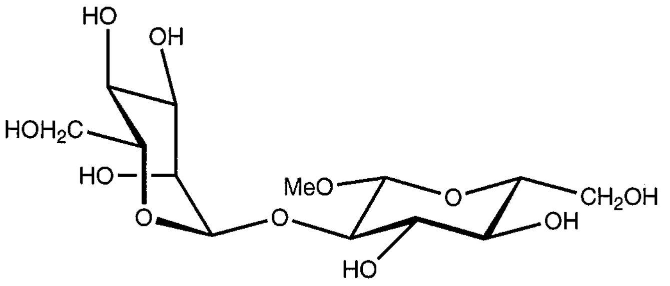

Figure 1. Schematic drawing of α-D-Man*p*-(1 → 2)-β-D-Glc*p*-OMe.

Davidon–Fletcher–Powell algorithm (HSEA) or steepest descent followed by Newton–Raphson (CHARMm) algorithm at these regions led to low energy conformers. Heteronuclear coupling constants were calculated using the Karplus relationship as devised by Tvaroska *et al.* [5] for each saved conformation, and subsequently averaged.

NMR spectroscopy

α-D-Man*p*-(1 → 2)-β-D-Glc*p*-OMe was dissolved in D_2O to a concentration of 100 mM. NMR spectra were measured at 300 K on a Varian Unity 500 MHz NMR spectrometer. Measurement of long-range ^{13}C, ^{1}H coupling constants were performed using a gradient enhanced version for ^{13}C site selective excitation as devised by Nishida *et al.* [6] A spectral width of 1200 Hz was sampled with 8192 data points using 3800 transients for each selective excitation. The FID was processed using Varian VNMR software. Zero-filling eight times and multiplication of the FID with an exponential weighting function with a line broadening of 0.3 Hz was applied prior to Fourier transformation. The *J*-doubling procedure used eight delta functions in the frequency domain. [7, 8]

Results and discussion

The conformational flexibility of α-D-Man*p*-(1 → 2)-β-D-Glc*p*-OMe has been investigated using MMC and LD simulations in which different force fields were employed. Either technique can be used for conformational search. The former is focused on averaged properties of a system whereas the latter also readily gives information on time scales for various processes.

The HSEA force field, in which sugar residues are kept rigid, leads to a more restricted region that is populated in conformational space than is the case for the CHARMm-based force field where all degrees of freedom are allowed to vary during the dynamics simulation (Figure 2). The populated region(s) are similar in both cases, although for HSEA only one low energy minimum is observed (Figure 3a). Four major energy minima are identified in the CHARMm force field, three of which differ by only a few tens of a kcal/mole.

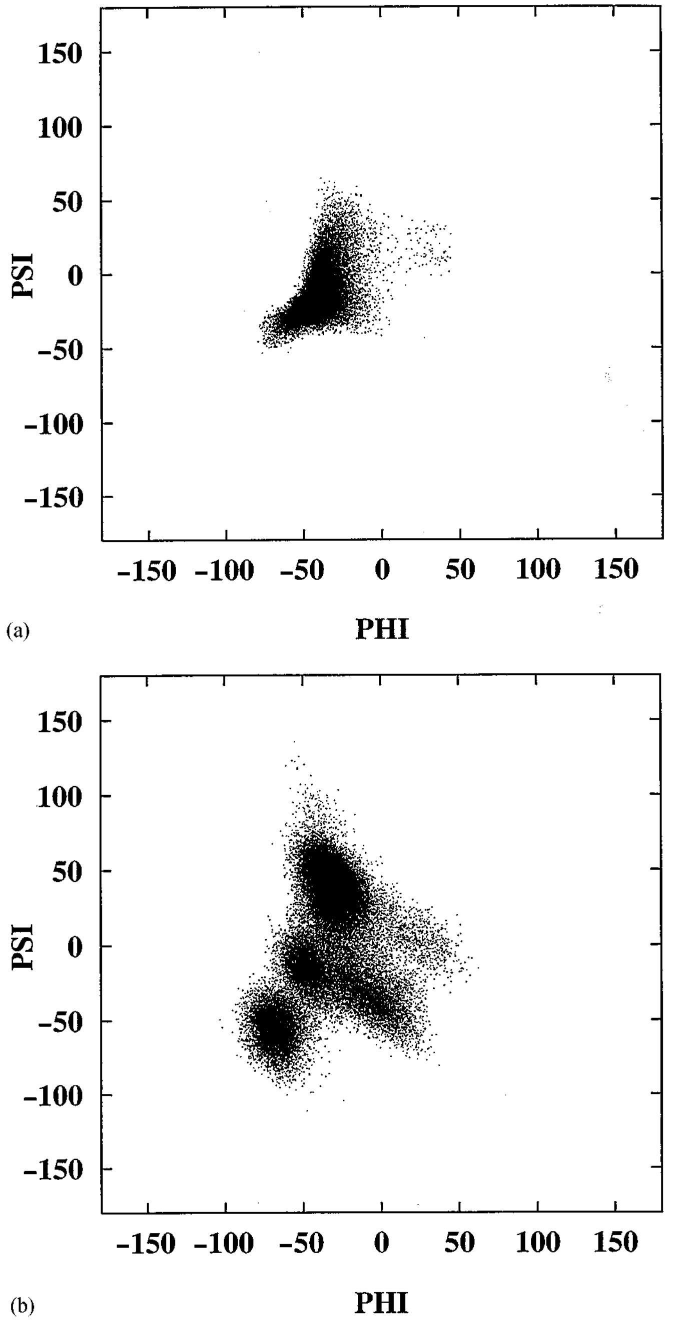

Figure 2. Scatter plots from MMC (a) and LD (b) simulation of α-D-Man*p*-(1 → 2)-β-D-Glc*p*-OMe.

An additional energy minimum, ca. 4 kcal/mole higher in energy is also sampled during the dynamics simulations (Table 1).

For the *ϕ* dihedral angle the exo-anomeric effect governs the major populated states. In the LD simulation, the *ψ* dihedral angle is allowed to vary to a larger extent. For comparison of flexibility the root-mean-square deviation values from the LD simulations are significantly larger than

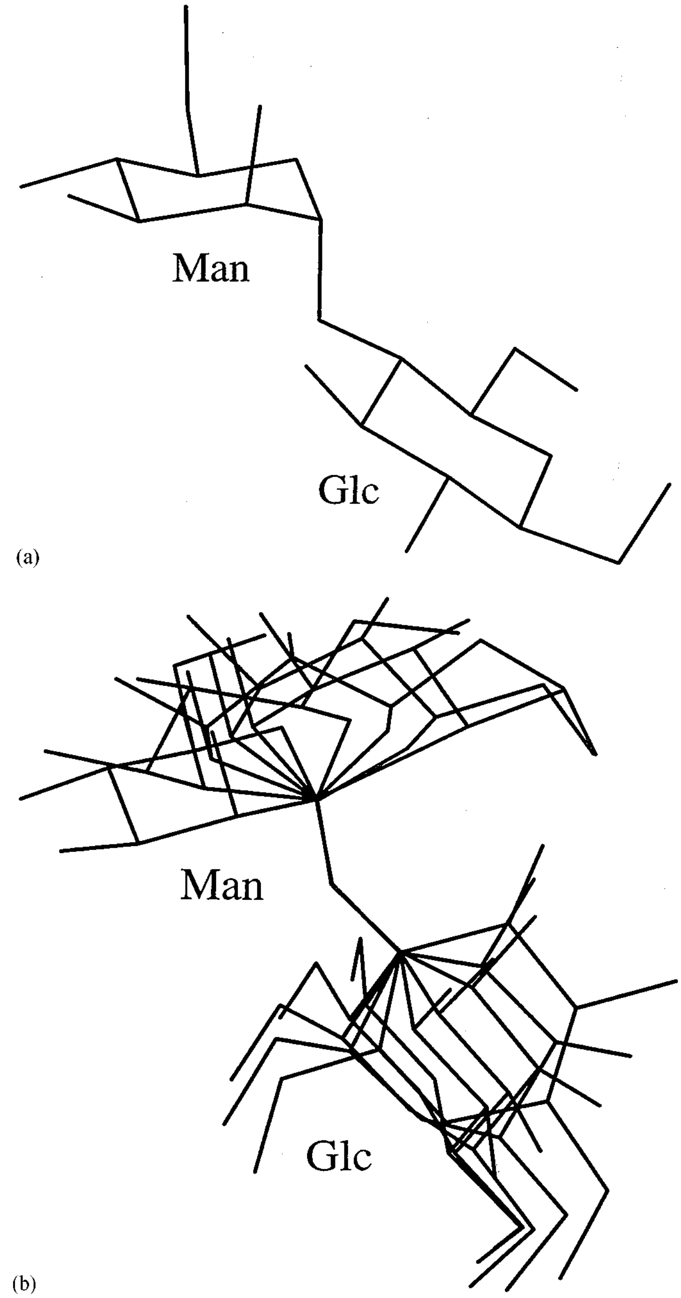

Figure 3. Global energy minimum conformer of *α*-D-Man*p*-(1 → 2)-*β*-D-Glc*p*-OMe employing the HSEA force field (a) and overlay of the five CHARMm conformers based on C1′, O2 and C2 (b).

those from the MMC simulations, namely for LD: $\phi = 22°$, $\psi = 42°$; and for MMC: $\phi = 12°$, $\psi = 17°$. To visualize the conformational flexibility of the disaccharide an overlay of the five CHARMm conformers from Table 1 is shown in Figure 3b. The overlay has been performed on the three atoms at the glycosidic linkage between the two monosaccharides. Thus, the conformational flexibility along both ϕ and ψ can be seen.

Table 1. Torsion angles for energy minimized structures and the crystal structure of *α*-D-Man*p*-(1 → 2)-*β*-D-Glc*p*-OMe

Conformation	ϕ	ψ	*Energy differences (kcal/mole)*
CHARMm I	– 33°	45°	0.0
CHARMm II	– 51°	– 12°	0.0
CHARMm III	– 70°	– 55°	0.3
CHARMm IV	– 2°	– 38°	1.5
CHARMm V	39°	– 1°	3.7
HSEA	– 43°	– 16°	
X-Ray	– 63°	– 29°	

The global energy minimum for the HSEA force field is similar to the CHARMm II energy minimum, i.e. the one enclosed by the three other conformations significantly populated. At this point the X-ray crystal structure of the disaccharide [9] can be compared to the accessible conformational space from the molecular mechanics calculations. The crystal structure conformation (Table 1) is approximately in between the CHARMm II and CHARMm III conformers and from the scatter plots it can be identified that the conformation of the crystal structure in both force fields is on the border of the conformational space as given by the molecular mechanics simulations. Thus, the crystal structure is observed at a low energy region on the Ramachandran maps, although not at a major local energy minimum on the map.

The LD simulations used to search conformational space also give additional information. The trajectories of the ϕ and ψ dihedral angles (Figure 4) show that most often transitions are correlated. A number of transitions between different energy wells occur during a 5 ns simulation, i.e. there are subnanosecond transitions. Thus, for the below discussion on coupling constants we conclude that the present LD simulations, in total 10 ns, have sampled the conformational space rather well, although significantly longer simulations are needed to reduce statistical errors in *eg* transition rates.

In conformational studies of biomolecules in solution the major source of experimental information based on NMR spectroscopy relies on the nuclear Overhauser effect and on spin–spin coupling constants. For carbohydrates a Karplus type relationship has been devised for the glycosidic linkage atoms. [5] This is a heteronuclear three-bond correlation between carbon and proton. We have measured these $^{3}J_{\mathrm{C,H}}$ values which are related to the ϕ and ψ dihedral angles. The selective excitation at the resonance for C2 led to the subsequent extraction of a $^{3}J_{\mathrm{H1'\text{–}C2}}$ value of 3.4 Hz (Table 2). In the same way a $^{3}J_{\mathrm{C1'\text{–}H2}}$ value of 5.4 Hz could be obtained. We estimate that the accuracy in the measured long-range coupling constants are better than $\pm$ 0.2 Hz. From the MMC and LD simulations the averaged

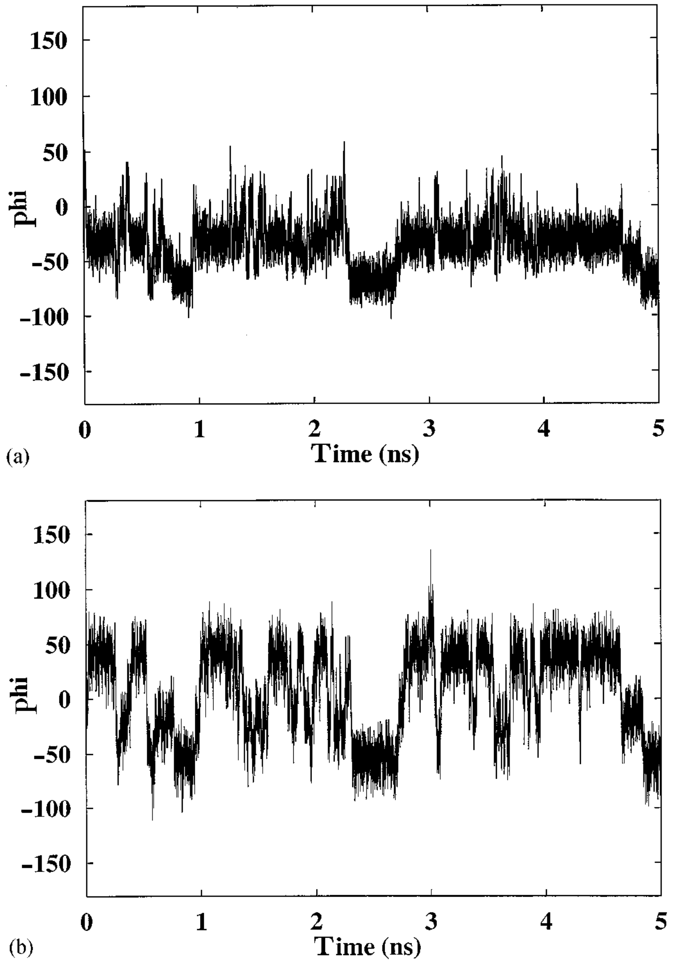

Figure 4. LD trajectories of title compound from one of the 5 ns simulations showing the dihedral angles ϕ and ψ as a function of time.

Table 2. Calculated and measured *trans*-glycosidic long-range heteronuclear coupling constants (Hz) for α-D-Man*p*-(1 → 2)-β-D-Glc*p*-OMe

Method	$^3J_{H1'-C2}$	$^3J_{C1'-H2}$
MMC	3.5	5.4
LD	3.6	5.6
NMR	3.4	5.4

long-range heteronuclear coupling constants across the glycosidic linkage were calculated. Both force fields show excellent agreement with the experimental data. Since the differences between the *J*-values calculated in the two force fields are on the same order as the experimental error, no distinction of a preferable force field can be drawn. In a previous study [10] employing a similar approach for 2- and 3-substituted disaccharides, the agreement between simulated and experimental data was not as good as in the present case. Calculation of $^3J_{C,H}$ values from the crystal structure led to 1.4 and 4.3 Hz for ϕ and ψ, respectively. Thus, the solid state structure differs from the averaged one in solution.

In conclusion, the conformational flexibility of α-D-Man*p*-(1 → 2)-β-D-Glc*p*-OMe is lower with the HSEA force field than with the CHARMm-based forced field. The overall three-dimensional structure is not significantly dependent on the force field, with both predicting a similar three-dimensional shape of the molecule. The crystal structure has a conformation which is sampled by the molecular mechanics simulations. In the LD simulations subnanosecond transitions occur between major low energy regions. Calculated heteronuclear long-range *trans* glycosidic coupling constants from the MMC and LD trajectories show excellent agreement for the disaccharide compared to those measured by NMR spectroscopy.

Acknowledgements

This work has been supported by a grant from the Swedish Natural Science Research Council. We thank the Swedish NMR Centre for putting NMR facilities at our disposal.

References

1 Jansson P-E, Kenne L, Persson K, Widmalm G (1990) *J Chem Soc Perkin Trans* **1**: 591–8.
2 Thøgersen H, Lemiux RU, Bock K, Meyer B (1982) *Can J Chem* **60**: 44–57.
3 Stuike-Prill R, Meyer B (1990) *Eur J Biochem* **194**: 903–19.
4 Venable RM, Pastor RW (1988) *Biopolymers* **27**: 1001–14.
5 Tvaroska I, Hricovoıíni M, Petráková E (1989) *Carbohydrate Res* **189**: 359–62.
6 Nishida T, Widmalm G, Sándor P (1996) *Magn Reson Chem* **34**: 377–82.
7 McIntyre L, Freeman R (1992) *J Magn Reson* **96**: 425–31.
8 del Rio-Portilla F, Blechta V, Freeman R (1994) *J Magn Reson Ser A* **111**: 132–5.
9 Eriksson L, Stenutz R, Widmalm G (1997) *Acta Cryst* **C53**: 1105–7.
10 Hardy BJ, Bystricky S, Kovac P, Widmalm G (1997) *Biopolymers* **41**: 83–96.

Received 9 September 1996, revised 8 December 1996, accepted 11 March 1997